11th World Congress on Computational Mechanics (WCCM XI)
5th European Conference on Computational Mechanics (ECCM V)
6th European Conference on Computational Fluid Dynamics (ECFD VI)
E. Oñate, J. Oliver and A. Huerta (Eds)

EVALUATION OF AN IMMERSED BOUNDARY METHOD FOR SOLVING THE FLUID STRUCTURE INTERACTION PROBLEM IN REFRIGERATION COMPRESSOR VALVES

JOSÉ L. GASCHE*, FRANCO BARBI†

* UNESP-Univ. Estadual Paulista, Department of Mechanical Engineering
Av. Brasil Centro 56
15385-000 Ilha Solteira, SP, Brazil
gasche@dem.feis.unesp.br, www.dem.feis.unesp.br

† UFU-Federal University of Uberlândia, Department of Mechanical Engineering
Campus Santa Mônica – Bloco M1
34800-902 Uberlândia-MG, Brazil
frcbarbi@gmail.com, www.mecanica.ufu.br/laboratorios/mflab

Key Words: *Immersed Boundary Method, Fluid-Structure Interaction, Compressor, Valve.*

Abstract. In refrigeration compressors, the suction and discharge valves are responsible for the retention of the refrigerant from the suction chamber to the cylinder and passage from the cylinder to the discharge chamber. As the opening and closing of the valves are caused by the forces produced by the refrigerant flow, the understanding of the flow through the valve is of fundamental importance in order to enhance the efficiency of the valve system. The numerical simulation of the flow is an efficient method to perform this task. Due to the complex geometry usually found in this type of valve, simplified geometries have been used to represent the valve, particularly the radial diffuser. This work presents a numerical simulation of the unsteady flow through a more realistic geometric model for the suction valve including the movement of the reed. An Immersed Boundary Method (IBM) with the Multi-Direct Forcing Scheme is used to represent the valve geometry and to solve the 3D unsteady flow for an imposed angular movement to the reed. An adaptive mesh dynamically refined is used for representing the flow domain. The governing equations are solved by a projection method, using a semi-implicit second-order scheme for time integration. The systems of algebraic equations are solved by a Multigrid-Multilevel technique. Results for pressure and velocity fields and for pressure profiles on the reed surface were obtained for Reynolds number varying from 1,000 to 8,000. The results show that the IBM is a very good alternative for solving the flow through reed type valves with complex geometry.

1 INTRODUCTION

The valve is one of the main components of hermetic compressors because it controls the mass flow rate through the compressor. The opening and closing movements of the valve are governed by the pressure difference applied by the refrigerant flow over the reed, as shown in

Figure 1. Therefore, it is essential to fully understand the flow through the valve in order to improve its design and to enhance the overall efficiency of the compressor.

Several studies have been carried out to characterize the main features of the flow through the valve, specially using the radial diffuser as a valve model. Numerical solutions for incompressible laminar and turbulent flows have been performed [1-8] as well as many experimental works [9-14].

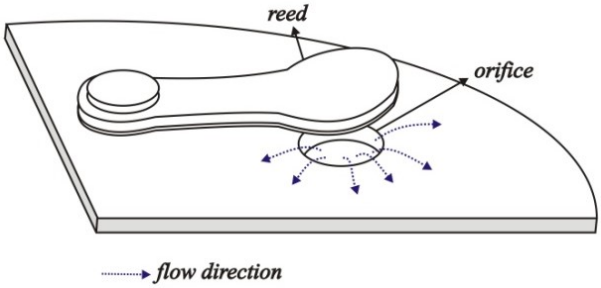

Figure 1:. Scheme of the valve reed.

One of the main challenges for modeling this problem is the complexity of the valve geometry. Because of this reason, simpler geometries have been adopted, specially the radial diffuser. The treatment of the valve reed movement is another challenge for the current computational fluid dynamics methods. The use of body-fitted meshes, where the computational mesh is set to fit to the body, introduces several computational penalties once that, for each displacement of the valve reed, the mesh must be updated for the discretization of the new computational domain. This procedure requires extensive computational resources.

An alternative method to accomplish the same task is the Immersed Boundary Method (IBM). The Immersed Boundary Method (IBM) introduced by Peskin [15] has been used successfully for solving flow problems in complex geometries presenting moving boundaries, especially for problems involving fluid-structure interaction. Therefore, this method is a natural procedure for solving the fluid-structure interaction occurring in valve systems. This method uses a Cartesian fixed grid (Eulerian grid) for solving the flow equations and models any immersed boundary using a moving Lagrangian grid. The immersed boundary is recognized through the addition of a force field (Lagrangian force field) in the momentum equations.

Lacerda [16] and Rodrigues [17] have used the IBM to simulate the two-dimensional incompressible flow through a radial diffuser representing the valve system. Lacerda [16] used the Virtual Physical Model (VPM) introduced by Lima e Silva [18] to calculate the Lagrangian force only to represent the valve seat. The results obtained by Lacerda agreed very well with experimental data. Rodrigues [17] used the same model used by Lacerda [16] to calculate the force field, but applied it to analyze the flow through a radial diffuser with moving frontal disc. Rodrigues concluded that the method was able to represent well the movement of the frontal disc.

In this work, the flow through a suction valve model is numerically simulated considering a real geometry to the valve. In order to accomplish this task a three-dimensional model was used to solve the incompressible flow through the suction valve, including the reed movement.

2 NUMERICAL METHOD

A three-dimensional, unsteady, incompressible, and isothermal flow of a Newtonian fluid is considered to solve the flow through the suction valve model. The governing equations (in Cartesian coordinates) are the mass conservation and the momentum equations, given by:

$$\nabla \cdot \mathbf{u} = 0 \tag{1}$$

$$\rho\left(\frac{\partial \boldsymbol{u}}{\partial t} + \boldsymbol{u} \cdot \nabla \boldsymbol{u}\right) = -\nabla p + \nabla \cdot \left[\mu\left(\nabla \boldsymbol{u} + \nabla \boldsymbol{u}^T\right)\right] + \boldsymbol{f} \tag{2}$$

where **u** represents the vector velocity field, p is the pressure, and ρ and μ are the density and the viscosity, respectively. The term $\boldsymbol{f}$ corresponds to the Eulerian force density field, which is responsible for representing the immersed boundary inside the flow. The Eulerian force is calculated through the distribution of the Lagrangian interfacial force, $\boldsymbol{F}$, by using the following equation:

$$\boldsymbol{f}(\boldsymbol{x}) = \int_{\Gamma} \boldsymbol{F}(\boldsymbol{X}) D(\boldsymbol{x} - \boldsymbol{X}) \Delta V \tag{3}$$

where $\boldsymbol{x}$ is the position of the Eulerian point, $\boldsymbol{X}$ the position of the Lagrangian point, ΔV the discrete volume for each Lagrangian point, Γ the Lagrangian domain, and $D(\boldsymbol{x}\text{-}\boldsymbol{X})$ is the distribution function having Gaussian function properties.

Several models to calculate the Lagrangian force, $\boldsymbol{f}$, have been developed [19]. In this work, the Multi-Direct Forcing proposed by Wang [20] is used to calculate the interfacial Lagrangian force. This method iterates a direct forcing process at the Eulerian points close to the immersed boundary to guarantee the desired velocity at the boundary. The procedure involves the following steps:

- Calculation of the velocity at the Lagrangian points using the distribution function:

$$\boldsymbol{U}^{t,i} = \sum_{\Gamma} D(\boldsymbol{x} - \boldsymbol{X}) \boldsymbol{u}^{\mathrm{t,i}}(\boldsymbol{x}) \Delta V \tag{4}$$

- Calculation of the Lagrangian force density, $\boldsymbol{F}$:

$$\boldsymbol{F}^i(\boldsymbol{X}, t) = \rho\left(\frac{\boldsymbol{U}^{t+\Delta t} - \boldsymbol{U}^{t,i}}{\Delta t}\right) \tag{5}$$

- Distribution of the Lagrangian force density to the Eulerian points through the distribution function:

$$\boldsymbol{f}^i(\boldsymbol{x}, t) = \sum_{\Gamma} D(\boldsymbol{x} - \boldsymbol{X}) \boldsymbol{F}^i(\boldsymbol{X}, t) \Delta V \tag{6}$$

- Update of the velocity field after forcing:

$$\boldsymbol{u}^{\mathrm{i+1}} = \boldsymbol{u}^{\mathrm{i}} + \frac{\Delta t}{\rho} \boldsymbol{f}^i(\boldsymbol{x}, t) \tag{7}$$

In the second step, $\boldsymbol{U}^{t+\Delta t}$ refers to the desired velocity at the immersed boundary. These four steps are repeated until $\boldsymbol{U}=\boldsymbol{U}^{t+\Delta t}$. The force acting on the immersed boundary can be calculated by:

$$\boldsymbol{F}(\boldsymbol{X},t)=\sum_{i=1}^{NF}\boldsymbol{F}^{i}(\boldsymbol{X},t) \tag{8}$$

where *NF* is the number of Multi-Direct Forcing cycles.

The mesh used consists in sequences of nested, progressive finer rectangular grid patches, as exemplified by Figure 2. The refinement strategy is based on the position of Lagrangian points and on the vorticity field [21]. The finest level of refinement is set for regions close to the Lagrangian points, while in other regions the refinement level is set considering the maximum vorticity value. The mesh dynamically adapts itself to the flow while the immersed boundary is represented by the finest level. Figure 2 shows an immersed boundary represented by the Lagrangian domain covered by the finest level of the Eulerian domain as an example.

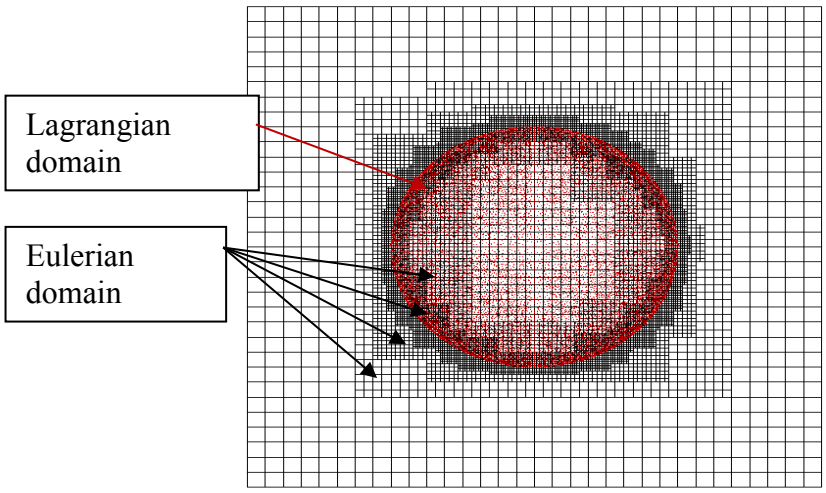

Figure 2: Example of the Lagrangian domain covered by the finest level of grid patches.

The temporal discretization of Equation (2) is based on the IMEX (Implicit-Explicit) scheme, a second order scheme described by Ascher [22]. This method allows the use of time-advance schemes as the SBDF (Semi-Backward Difference Formula), MCNAB (Modified Cranck-Nicolson Adams-Bashforth), CNAB (Cranck-Nicolson Adams-Bashforth), and CNLF (Cranck-Nicolson Leap-Frog). The central difference scheme (CDS) is used to discretize the spatial terms of the equation. The Projection Method is used for the solution of the pressure-velocity coupling, while the algebraic linear systems are solved by a multigrid technique. The Large Eddy Simulation (LES) with the standard Smagorinsky model was used to treat the turbulence phenomenon.

The geometry of the valve is depicted in Figure 3. The IBM can reduce substantially the difficulty to represent complex geometries because it is not necessary to adapt the grid to the immersed boundaries.

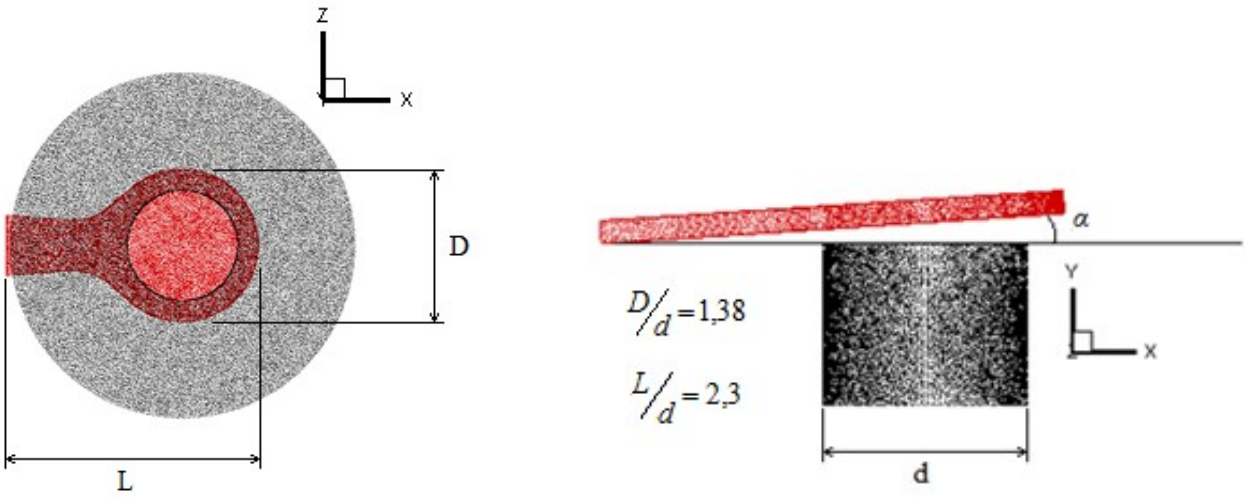

(a) – Top view (b) – Side view

Figure 3: Valve model.

For this initial work, the reed movement is imposed by a sine type function that describes the angle variation, α, with time (φ=3π/48, A=π/24, and ω=1.5 rad/s),

$$\alpha(t) = \varphi + A \sin\left(\omega t + \frac{3\pi}{2}\right) \tag{9}$$

In Equation (9), A stands for the angular movement amplitude, φ is the minimum angle and ω is the angular velocity. The mass flux in the feeding orifice is imposed by a group of points, indicated in Figure 4. For these Lagrangian points, velocity $\boldsymbol{U}^{t+\Delta t}$ in Equation (5) is taken as the desired velocity in the feeding orifice. Figure 5 shows the entire domain and the boundary conditions. The Eulerian domain is a 12d edge cube covered by 6 refinement levels, where the coarser level is formed by 24 cells in each direction.

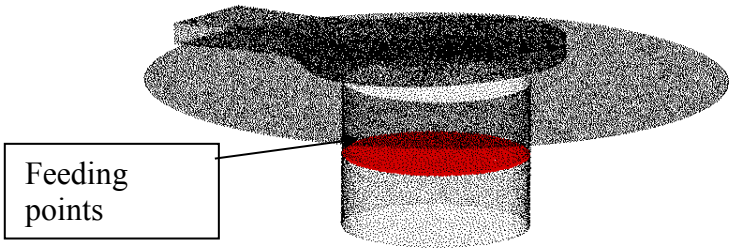

Figure 4: Tri-dimensional model highlighting the group of points imposing the velocity in the feeding orifice.

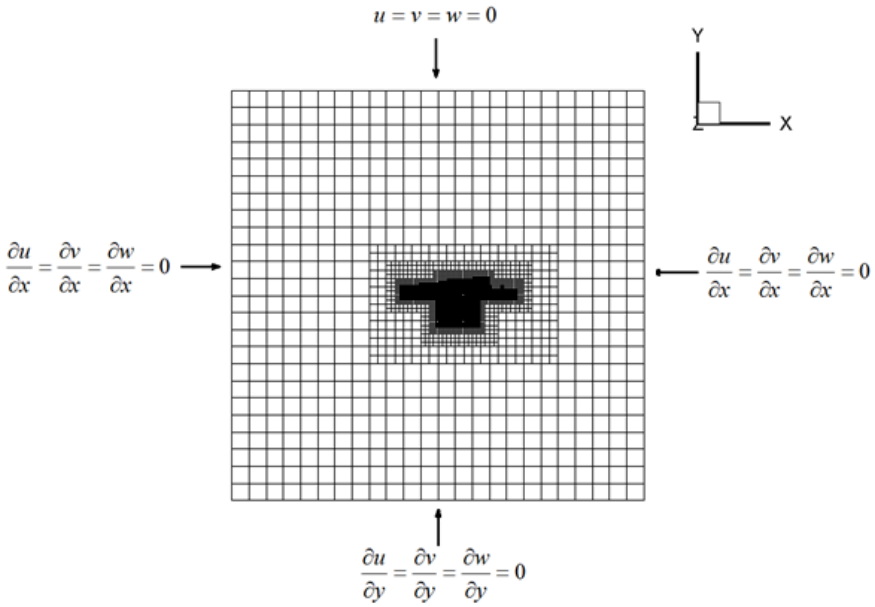

Figure 5: Computational domain and boundary conditions.

The results were obtained by using 73.038 nodes for the Lagrangian grid, while the Eulerian grid is composed of about 3.000.000 nodes, considering that the number of nodes varies with the effect of the adaptive refinement. The dimensionless parameters used to present the results are the Reynolds number, $Re_d=\rho U_a d/\mu$, the dimensionless pressure, $P^*=P/(\rho U_a^2/2)$, and the dimensionless time, $t^*=U_a t/d$, where U_a is the average velocity at the orifice and d is the feeding orifice diameter. In this work, the representation of the immersed boundary with no-slip condition is evaluated by calculating the maximum L_2 norm of the velocity vector at each Lagrangian point in the immersed boundaries. The L_2 norm is defined by

$$L_2 = \frac{1}{N}\sqrt{\sum_{i=1}^{N}[(u_i - u_{ki})^2 + (v_i - v_{ki})^2 + (w_i - w_{ki})^2]} \tag{13}$$

where u_i, v_i, and w_i are the Eulerian velocity components, and u_{ki}, v_{ki}, and w_{ki} are the prescribed Lagrangian velocity components at the Lagrangian points describing the immersed boundaries.

3 RESULTS

First of all, the methodology was validated by solving the steady flow through a radial diffuser with s/d=0.07 (dimensionless gap between discs), D/d=1.2 (ratio between the diameter of the frontal disc, D, and orifice, d), for Re_d=2,500. Figure 6 presents the results for the pressure profile on the frontal disc comparing with the results obtained by using a Finite Volume Method (traditional method) and experimental results. The results were obtained for two different meshes with refinement ratio equal to two, so that it was possible to estimate the numerical error by using Richardson extrapolation. One can see a good agreement among the results.

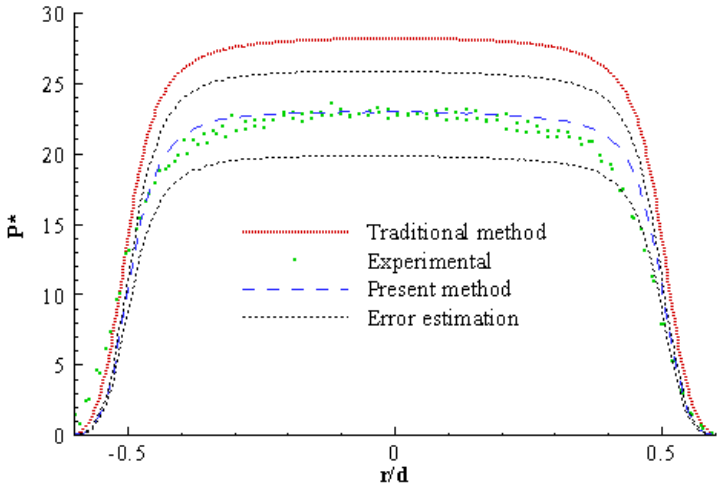

Figure 6: Validation of the methodology (for NF=6)

The methodology was then tested for moving reed for Reynolds number varying from 1,000 to 8,000 using a time-step of the order of 10^{-4} and NF=3. Dimensionless pressure distributions on the reed surface are plotted using the coordinate system indicated in Figure 7.

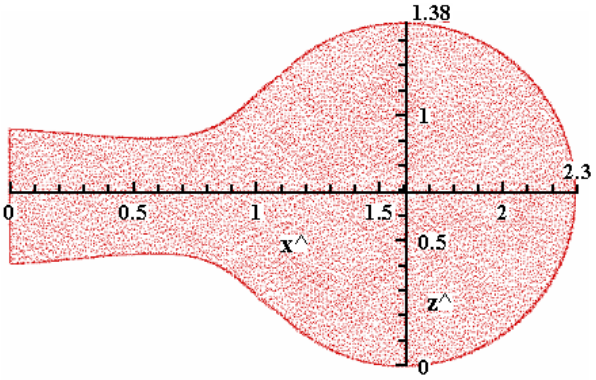

Figure 7: Reed surface with dimensionless variables x^=*x/d* and z^=*z/d*.

The L_2 norm is a very important parameter in this methodology because it defines the quality of the no-slip condition at the immersed boundaries. It was observed that the value of the L_2 norm varies with the velocity of the reed. Its maximum value was 0.08 for α=11.25º, which is the position of maximum reed velocity, while the minimum value (0.01) was obtained for α=3,75º and α=18.25º, where the reed velocity is zero. These values showed to be sufficient to obtain the no-slip condition at the surfaces of the reed. In order to obtain lower norm values, the number of cycles of the multi-direct forcing (NF) should be increased.

Figure 8 show pressure profiles for the opening movement of the reed in the *x* direction for Re_d=3,000. One can observe that the pressure profiles in the *x* direction for the several angles have the same pattern in general. As expected, the larger pressures occur in the circular region of the reed (1.0<x^<2.3). The pressure decreases from the center of the circular region of the reed (x^=1.6) to the exit of the flow due to the acceleration of the flow when it enters the

diffuser region (region between the reed and the seat). There is a small increase in the pressure for x^ smaller than 1.0, mainly for α=6.25°, due to the decrease in the velocity after a recirculation bubble formed due to the acceleration of the flow. After this region the pressure decreases again due to friction effects. In addition, one can notice that the pressure decreases for increasing angles up to α=11.25° due to the reduction of the friction forces of the flow in the diffuser region. For larger angles, the pressure starts increasing again owing to the deceleration of the reed. Figures 9 shows the velocity field at α=6.25° for the opening movement where one can see the recirculation bubbles at the exit of the orifice region (entrance of the diffuser region). In addition, one can observe the stagnation region at the center of the circular part of the reed, where the pressure presents the maximum values.

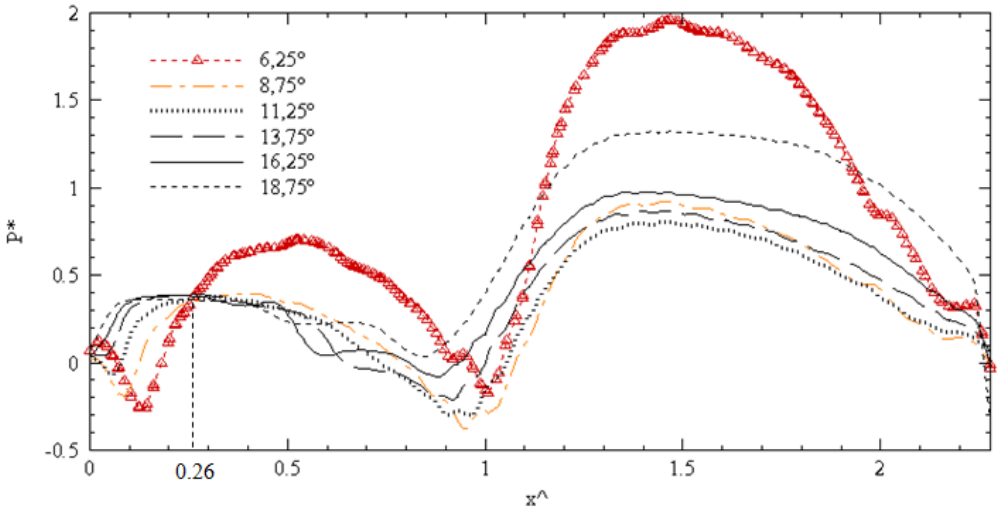

Figure 8: Pressure profile in the x direction for Re_d=3,000 (opening movement).

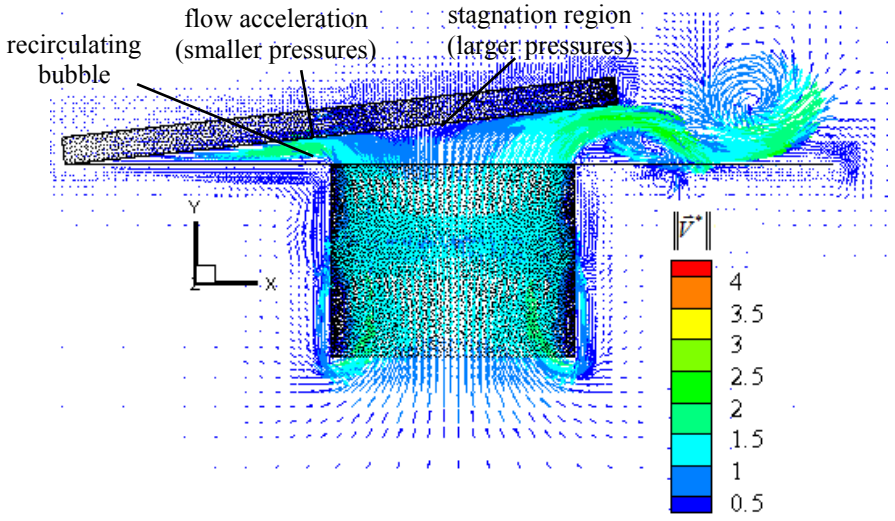

Figure 9: Velocity field for Re_d=3,000 in a x-y plane passing through the orifice center line (opening movement for α=6.25°).

Figure 10 shows similar results for Re_d=8,000. The general pattern of the pressure profiles are analogous, excepts for α=6.25°, in which one can see another pressure peak in the circular region of the read due to recirculating bubbles at the exit of the flow as can be seen in Figure 10(c). Figure 11 depicts the pressure profiles at α=6.25° for Reynolds number varying fron 1,000 to 8,000.

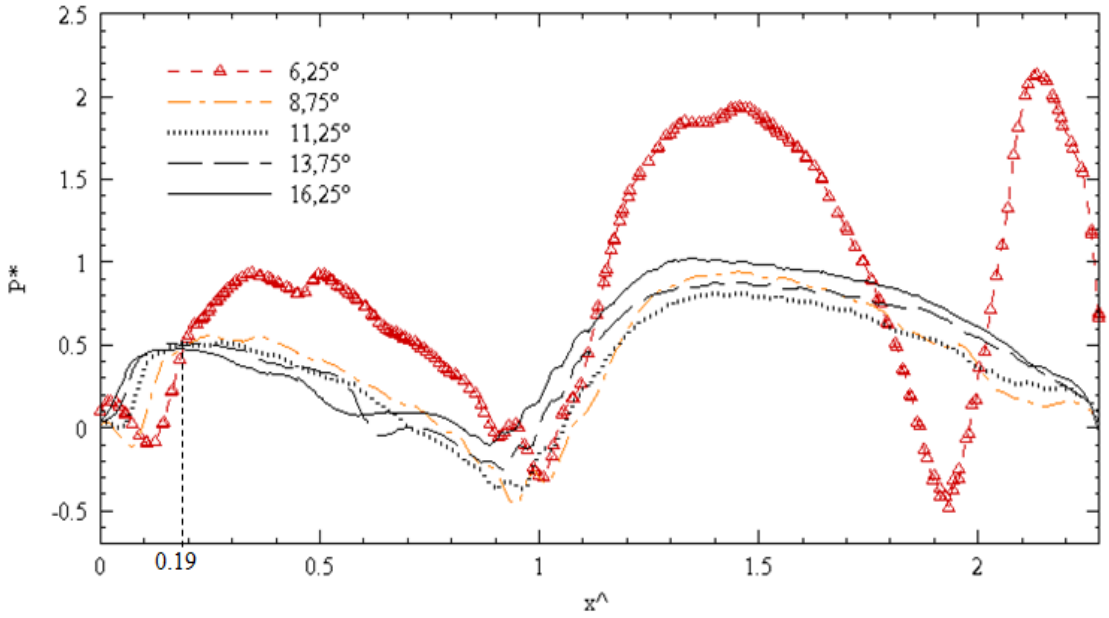

Figure 10: Pressure profile in the x direction for Re_d=8,000 (opening movement).

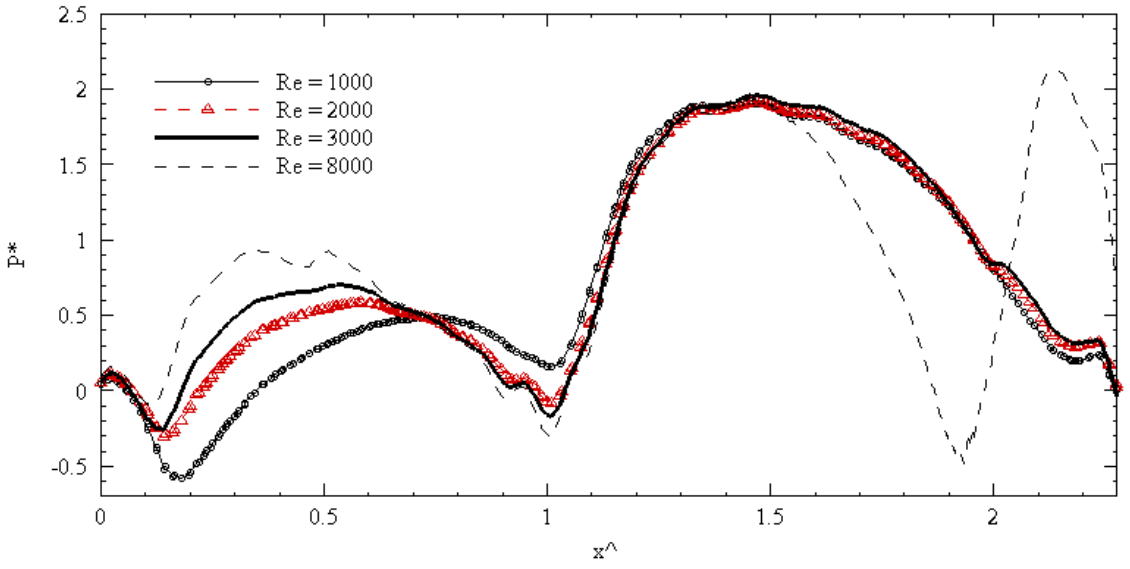

Figure 11: Pressure profile in the x direction for the opening movement for α=6.25°.

Figure 12 shows pressure fields for Reynolds numbers equal to 1,000, 3,000, and 8,000. One can note that the oscillations appearing in the pressure profiles on the reed surface (Figures 8, 10, and 11) are due to the formation of eddies in the diffuser region. As expected, the ddy formation increases as the Reynolds number also increase.

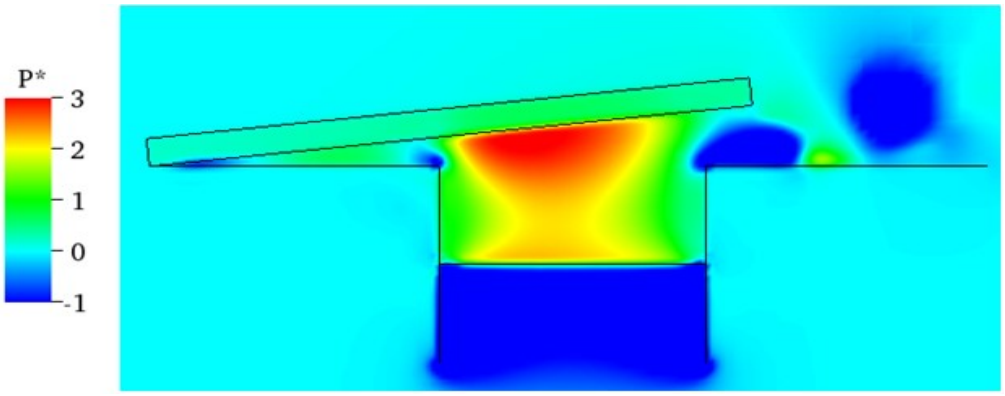

(a) Re_d=1,000

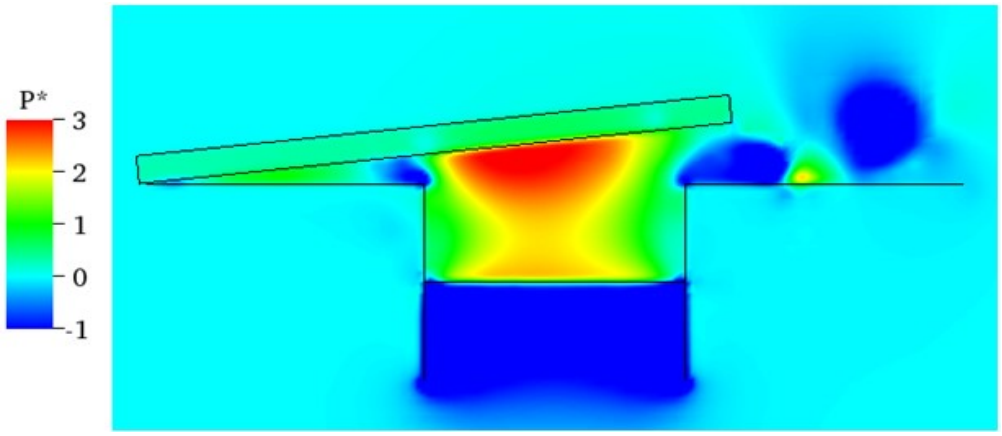

(b) Re_d=3,000

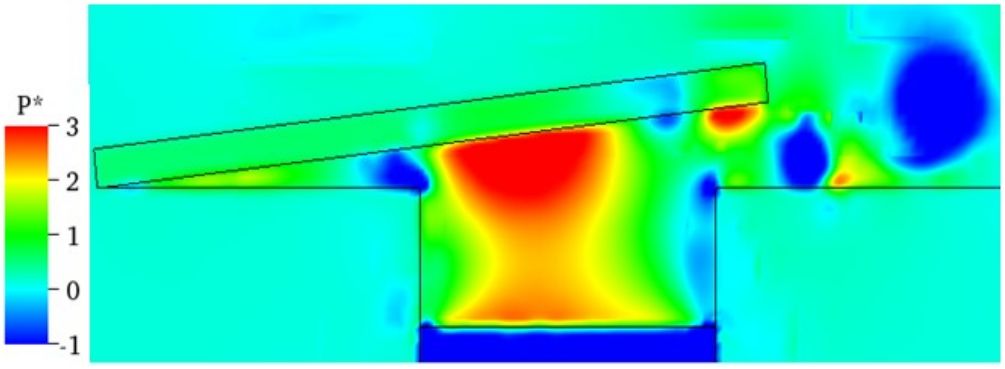

(c) Re_d=8,000

Figure 12: Pressure field in a x-y plane passing through the orifice center line (opening movement for α=6.25°).

4 CONCLUSIONS

A numerical methodology for simulating the flow in a more realistic model for reed type valves of reciprocating compressors is presented in this paper. The Immersed Boundary Method (IMB), which is an alternative method for solving problems with moving boundaries, is used to represent the geometry of the reed. In this first application of the method, the angular opening and closing movement of the reed is imposed by a sinusoidal function. Results for pressure profiles on the reed surface, velocity field and pressure field are presented for the opening movements of the reed and showed physical consistence with other results usually found in the literature. The main conclusion of the paper is that the IBM is a good alternative for solving the flow through reed type valves with complex geometry. The next step of the work is to introduce a structural model for the valve and compute the fully fluid-structure interaction.

REFERENCES

[1] Hayashi, S., Matsui, T. e Ito, T., 1975, Study of Flow and Thrust in Nozzle-Flapper Valves, *Journal of Fluids Engineering*, vol. 97, p. 39-50.

[2] Raal, J.D., 1978, Radial Source Flow Between Parallel Disks, *Journal of Fluid Mechanics*, vol. 85, p. 401-416.

[3] Piechna, J.R. and Meier, G.E.A., 1986, Numerical Investigation of Steady and Unsteady Flow in Valve Gap, *International Compressor Engineering Conference at Purdue*.

[4] Ferreira, R. T. S., Prata A. T., Deschamps C. J., 1989, Pressure distribution along valve reeds of hermetic compressors, *Experimental Thermal and Fluid Science*, vol. 2, no. 2: p. 201-207.

[5] Gasche, J.L., Ferreira, R.T.S., Prata, A.T., 1992, Pressure distribution along eccentric circular valve reed of hermetic compressors, *12th Purdue Int. Compressor Technology Conference*, West Lafayette, USA, pp. 1189-1198.

[6] Possamai, F. C., Ferreira R. T. S., Prata, A. T., 2001, Pressure distribution in laminar radial flow through inclined disks, *International Journal of Heat Fluid Flow,* vol. 22, no. 4: p. 440-449.

[7] Deschamps, C.J., Ferreira, R.T.S. e Prata, A.T., 1996, Turbulent Flow Through Reed Type Valves of Reciprocating Compressors, ASME, *International Mechanical Engineering Congress*, Atlanta, EUA.

[8] Colaciti, A. K, López, L. M. V., Navarro, H. A., Cabezas-Gómez, L., 2007, Numerical Simulation of a Radial Diffuser Turbulent Airflow, *Applied Mathematics and Computation*, vol. 189, p. 1491-1504.

[9] Wark, C.E., Foss, J.F., 1984, Forces Caused by the Radial Out-Flow Between Parallel Disks, *Journal of Fluids Engineering*, vol. 106, p. 292-297.

[10] Ferreira, R. T. S., Driessen, J. L., 1986, Analysis of the influence of valve geometric parameters on the effective flow and force areas, *International Compressor Engineering Conference at Purdue*, p. 632-646.

[11] Tabatabai, M., Pollard, A., 1987, Turbulence in Radial Flow Between Parallel Disks at Medium and Low Reynolds Numbers, *Journal Fluid Mech*., vol. 185, p. 483-502.

[12] Ervin, J.S., Suryanarayana, N.V. e Chai NG, H., 1989, Radial, Turbulent Flow of a Fluid Between Two Coaxial Disks, *Journal of Fluid Engineering*, vol. 111, p. 378-383.

[13] Gasche, J. L., 1992, Laminar flow through eccentric valves of refrigeration compressors, *MS. Dissertation, (in Portuguese)*, Federal University of Santa Catarina, Florianópolis-SC, Brazil, 149 p.
[14] Souto, L. E. M., 2002, Experimental investigation of turbulent flow in compressors , *MS. Dissertation, (in Portuguese),* Federal University of Santa Catarina, Florianópolis-SC, Brazil, 105 p.
[15] Peskin, C. S., 1972, Flow pattern around heart valves: a numerical method, *Journal of Computational Physics*, vol. 10, no. 2: p. 252-271.
[16] Lacerda, J., Gasche, J. L., 2010, Analysis of the Flow in Hermetic Compressor Valves Using the Immersed Boundary Method, *Interrnational Compressor Engineering Conference at Purdue*.
[17] Rodrigues, T. T., Gasche, J. L., Militzer, J., 2010, Flow Simulation Through Moving Hermetic Compressor Valves Using the Immersed Boundary Method, *Interrnational Compressor Engineering Conference at Purdue*.
[18] Lima e Silva, A. L. F., Silveira-Neto, A., Damasceno, J. J. R., 2004, Numerical simulation of two-dimensional flows over a circular cylinder using the immersed boundary method, *Journal of Computational Physics*, vol. 189, no. 2: p. 351-370.
[19] Mittal, R.; Iaccarino, G., 2005, Immersed boundary methods. *Annual Review of Fluid Mechanics***,** Palo Alto, v. 37, p. 239-261.
[20] Wang, Z., Fan, J., Luo, K., 2008, Combined Multi-Direct Forcing and Immersed Boundary for Simulating Flows with Moving Particles*, International Journal of Multiphase Flow* 34, p. 283-302.
[21] Roma, A. M., Peskin, C. S., Berger, M. J., 1999, An Adaptive Version of the Immersed Boundary Method, *Journal of Computational Physics* 153, p. 509-534.
[22] Ascher, U. M., Ruuth, S. J., Wetton, B., 1995, Implicit-Explicit Methods for Time Dependent Pde's., *SIAM (Soc. Ind. Appl. Math.) J. Numer. Anal*., vol. 32, p. 797.

ACKNOWLEDGEMENT

The authors acknowledge the support provided by FAPESP (Grant n° 2010/16837-9) and TECUMSEH do Brasil Ltda.